Unidirectional Cloaking Based on Metasurfaces with Balanced Loss and Gain

Dimitrios L. Sounas, Romain Fleury, and Andrea Alù

Phys. Rev. Applied **4**, 014005 — Published 16 July 2015

DOI: 10.1103/PhysRevApplied.4.014005

Unidirectional cloaking based on metasurfaces with balanced loss and gain

Dimitrios L. Sounas, Romain Fleury, and Andrea Alù*

Department of Electrical and Computer Engineering, The University of Texas at Austin, Austin, TX 78712, USA

*To whom correspondence should be addressed: alu@mail.utexas.edu

We prove that balanced loss/gain distributions provide an elegant path towards realizing loss-free unidirectional cloaks for objects much larger than the wavelength. By coating a scatterer with an ultrathin metasurface with balanced loss/gain, such as a Parity-Time (PT) symmetric metasurface in the special case of a symmetric scatterer, we show that it is possible to ideally cloak it from a particular direction. The passive portion of the cloak ensures that the incident power on the illuminated side of the object is fully absorbed, while the active portion radiates the required pattern on the opposite side, automatically synchronized with the impinging signal, eliminating shadows and making the object invisible. The proposed approach substitutes complex metamaterial cloaks and achieves cloaking with relaxed limitations on size, and in an ultrathin, loss-free and stable design. Beyond introducing a new venue to cloaking of large objects, our paper shows the unique potential for scattering manipulation introduced by structures with balanced loss and gain, pointing to a new direction in the field of PT-symmetric systems.

PACS: 42.30.Wb, 03.65.Nk, 11.30.Er, 42.24.Bs, 78.67.Pt

I. Introduction

Cloaking an object and making it undetectable to the impinging wave has attracted tremendous attention in the last decade: the advent of metamaterials [1] and the emergence of concepts such as transformation-optics [2],[3] and scattering cancellation techniques [4]-[7] have heated up the interest in camouflaging and invisibility. These metamaterial approaches aim at cancelling an object's scattering cross-section for any illumination direction, often at the expense of structural complexity and inherent limitations on bandwidth, electrical size of the object to be cloaked and overall scattering reduction [8],[9]. Nevertheless, there are many practical situations for which the direction of an impinging wave is known to a good degree, and an object needs to be made invisible only over a limited angular range. This fact has recently inspired the design of unidirectional cloaks [10]-[15], i.e., cloaks that are able to suppress the scattering for a particular incidence direction, relaxing the inherent constraints of full cloaking techniques. For example, based on the carpet-cloaking concept, Ref. [12] presented a unidirectional transformation-optics cloak with simplified material parameters, although still relying on anisotropic electric and magnetic materials. Using a different principle, Refs. [13]-[15] reported active cloaks based on the equivalence principle, in which the cloaked object is coated with antenna arrays supporting suitable electric and magnetic sources that can cancel the scattered field for a particular incident wave. Such designs rely on prior knowledge of both the amplitude and phase of the impinging wave, and usually require advanced signal processing networks [16].

In a different context, unidirectional invisibility has recently been studied as a unique property of one-dimensional (1D) parity-time (*PT*) symmetric structures [17]-[20]. *PT* symmetry is the invariance of a system under parity and time-reversal operations, and it has recently attracted significant attention because it can lead, quite unexpectedly, to non-Hermitian Hamiltonians with

real eigenvalues [21],[22]. Although the relevance of *PT* symmetry in quantum mechanics is still disputed [23], this is not the case for optical *PT* symmetry, which has already been reported in structures with balanced amounts of gain and loss [24]-[27], and is accompanied by unique phenomena, such as laser-absorber modes [28], enhanced non-reciprocity [29],[30], negative refraction [31], and sensing [32]. Unidirectional invisibility is known to arise in 1D *PT*-symmetric lattices, which can exhibit unitary transmission for forward and backward propagation directions, yet zero reflection for one propagation direction and non-zero reflection for the other one. The concept of *PT*-symmetric unidirectional invisibility was recently extended to two-dimensional geometries by applying coordinate transformations to a *PT*-symmetric cylindrical region [33],[34]. However, the invisibility achieved using this concept is imperfect and it requires the use of anisotropic electric and magnetic materials with loss and gain, which may be even more challenging to realize than the lossless anisotropic materials involved in conventional transformation-optics methods.

Here, we show that ideal unidirectional cloaking may be obtained, independent of the object size, using a single, ultrathin metasurface with balanced loss/gain. Our concept is partially inspired to the mantle-cloaking technique [5], a recently introduced cloaking mechanism based on homogeneous metasurfaces designed to suppress a large portion of the scattering from objects of limited electrical size. The conventional mantle cloaking approach was originally based on passive surfaces, although an extension to active inclusions was recently introduced in [35] with the goal of broadening its operational bandwidth. This technique is aimed at cancelling the first few scattering harmonics of the object to be cloaked by inducing suitable conduction currents on the admittance surface. Since the number of scattering harmonics determining the scattering properties of an object grows very fast with its electrical size, there is a fundamental limit on the

maximum size of objects that can be efficiently cloaked with one or a few homogeneous surfaces. In contrast, here we prove that, by surrounding a perfectly conducting (PEC) cylinder of arbitrary size with an inhomogeneous, ultrathin admittance surface with balanced loss/gain, it is possible to realize *identically zero* scattering for monochromatic waves propagating along the $+x$ direction (Fig. 1). The proposed approach is able to overcome the aforementioned limitations of conventional cloaking techniques, achieving total invisibility for objects, in principle of any size, with a single, ultrathin surface, yielding a recipe much simpler than transformation-optics cloaks, and potentially relaxing the constraints on bandwidth of passive cloaking approaches. In the following, after introducing the concept, we apply the proposed technique to circular and rhomboidal cylinders. We show that, for a small separation between the mantle surface and the object, the required surface admittance follows simple spatial profiles, which open an exciting path towards loss-free cloaking of objects with sizes significantly larger than the wavelength of operation.

II. Cloaking with metasurfaces with balanced loss/gain

Arguably, the simplest way to obtain full invisibility of an object illuminated by a plane wave consists in completely absorbing the incident power on one side of the structure (left-hand side in Fig. 1), and emitting the same signal, with same amplitude, phase and angular pattern, on the other side (right-hand side in Fig. 1). If we were to tackle this functionality with an ultrathin surface, the absorbing and emitting portions of such a metasurface should obviously have loss and gain, respectively. Consider first the 2D circularly symmetric scenario in Fig. 1, in which a perfectly conducting circular cylinder is surrounded by a cloaking ultrathin metasurface. In such a case, the required surface admittance Y_s is readily calculated from the boundary condition

$\mathbf{J}_s = Y_s \mathbf{E}_s$, where $\mathbf{E}_s$ and $\mathbf{J}_s$ are the electric field and current on the surface, respectively. The latter is given by $\mathbf{J}_s = \hat{\mathbf{r}} \times (\mathbf{H}_+ - \mathbf{H}_-)$, where $\mathbf{H}_+$ and $\mathbf{H}_-$ are the magnetic field at the exterior and interior side of the surface, respectively. For ideal invisibility, the only field outside the surface is the incident one, $\mathbf{E}_{\text{inc}} = E_0 e^{ikx} \hat{\mathbf{z}}$, yielding $\mathbf{E}_s = E_0 e^{ikd\cos\varphi} \hat{\mathbf{z}}$ and $\mathbf{H}_+ = -Y_0 E_0 e^{ikd\cos\varphi} \hat{\mathbf{y}}$, where Y_0 is the wave admittance in free space. For the calculation of $\mathbf{H}_-$, the exterior and interior fields are expanded in terms of cylindrical harmonics $J_n(kr)e^{in\varphi}$ and $Y_n(kr)e^{in\varphi}$ as

$$\begin{aligned} \mathbf{E}_{\text{ext}} &= \mathbf{E}_{\text{inc}} = \hat{\mathbf{z}} E_0 \sum_{n=-\infty}^{\infty} i^n J_n(kr) e^{in\varphi}, \\ \mathbf{E}_{\text{int}} &= \hat{\mathbf{z}} E_0 \sum_{n=-\infty}^{\infty} i^n [a_n J_n(kr) + b_n Y_n(kr)] e^{in\varphi}. \end{aligned} \tag{0}$$

The corresponding magnetic fields are found using Faraday's law, $\mathbf{H} = \nabla \times \mathbf{E} / (i\omega\mu_0)$, and the coefficients a_n and b_n are calculated by applying the boundary conditions for the electric field on the admittance surface and the PEC cylinder. After some straightforward algebraic manipulations, we find

$$Y_s = iY_0 \frac{2}{\pi kd} e^{-ikd\cos\varphi} \sum_{n=-\infty}^{\infty} i^n \frac{J_n(ka)}{J_n(kd)Y_n(ka) - J_n(ka)Y_n(kd)} e^{in\varphi}. \tag{1}$$

An interesting property of Y_s in Eq. (1) is that it satisfies the *PT*-symmetric condition $Y_s(\pi - \varphi) = -Y_s^*(\varphi)$. In fact, this is a general property of symmetric, lossless objects, such as the metallic circular cylinder in Fig. 1, illuminated by *PT*-symmetric fields, such as plane waves. Applying a *PT* transformation to such an object covered by an admittance surface $Y_s(\varphi)$ results in the same object covered by an admittance surface $-Y_s^*(\pi - \varphi)$. If $Y_s(\varphi)$ is selected so that the

object is invisible from a particular direction, the field outside the cloak is simply the plane wave impinging on the object. Since plane waves are *PT* symmetric, we conclude that $-Y_s^*(\pi-\varphi)$ must provide as well invisibility. If the impedance surface is unique, which was shown to be true in (1), $Y_s(\varphi)=-Y_s^*(\pi-\varphi)$, demonstrating that the required cloaking surface is *PT*-symmetric.

Eq. (1) can be substantially simplified in the limiting case $k(d-a)\ll 1$, i.e., for a thin spacer between the metasurface and the metallic cylinder. Taking the Taylor expansion of Y_s with respect to d around $d=a$, and keeping the terms up to the zeroth order, yields

$$\begin{aligned}\mathrm{Re}\{Y_s\} &\approx -Y_0\cos\varphi,\\ \mathrm{Im}\{Y_s\} &\approx -Y_0\left[\frac{1}{k(d-a)}-\frac{1}{2ka}\right].\end{aligned} \tag{2}$$

Eq. (2) has a simple physical interpretation in terms of geometrical optics: for $|\varphi|>\pi/2$ (lossy side of the mantle surface), $\mathrm{Re}\{Y_s\}$ is exactly equal to the characteristic admittance of a +*x*-propagating plane wave projected along the tangent to the cylinder's surface at the location φ. At the same time, the imaginary part of Y_s suppresses the local cylinder's reactance, since $-Y_0/[k(d-a)]$ is exactly opposite to the input susceptance of a shorted transmission line with length $d-a$, while the term $Y_0/(2ka)$ is related to the finite curvature of the cylinder. Therefore, the admittance surface realizes the necessary condition for ideal impedance matching between the mantle surface and the incident wave at any position $|\varphi|>\pi/2$ in a ray-picture approximation, and it consequently allows for full absorption of the incident power. This is visible in Fig. 2a, in which we show the electric field and power distribution for a cylinder with a diameter of four wavelengths covered by just the passive portion of the proposed surface,

conformal to the left-hand side of the cylinder ($|\varphi| > \pi/2$) at a distance $d - a = 0.01\lambda$ from its surface: all the incident signal is absorbed by the surface, resulting in zero back-scattering, but a large shadow is created at the right-hand side of the cylinder, making it detectable from the forward direction. This is the functionality of an ideal stealth surface, which absorbs the impinging wave and eliminates any reflection, but it is generally detectable from its shadow in the case of bi-static radar measurements, or from the dark spot that would create in an otherwise bright background in the case of mono-static radar measurements.

Eq. (2) suggests, however, that if we coat the back portion of the cylinder with the time-reversed version of this stealth passive surface, we may be able to realize ideal cloaking in a *super-stealth* configuration, where both backward and forward scattering are totally suppressed. Indeed, for $|\varphi| < \pi/2$ (gain side of the surface), $\mathrm{Re}\{Y_s\}$ is *opposite* to the characteristic admittance of an *x*-propagating plane wave on any of the cylinder's tangential planes. This condition leads to a locally infinite reflection coefficient, similarly to a semi-infinite transmission line terminated with an impedance opposite to the line's characteristic impedance, where self-sustained power emission (lasing) is supported. Emission without excitation does not arise in our scenario, as we prove below, due to the finite area covered by the gain medium: although the infinite local reflection coefficient ensures that an infinitesimal amount of power impinging on an infinitesimal section of the coated cylinder results in a finite radiated field, integrating this field all over the finite area of the object, yields a finite value for the total scattered field. Nevertheless, a weak signal with appropriate amplitude and phase in sync to the incident one, as the one leaking in the shadow region of Fig. 2a from the top and bottom of the cylinder, triggers the emission of a +*x*-propagating plane wave, cancelling the shadow effect created by the stealth portion of the surface. This is visible in Fig. 2b, which shows the electric field and the power

distribution of a fully-cloaked cylinder using the approximate ultrathin surface described in Eq. (2): the incident plane wave absorbed at the left-hand side of the cylinder is fully restored in amplitude and phase at its right-hand side, making the object fully undetectable, even in the forward direction. For comparison, Fig. 2c presents the electric field and power distribution for the case of a bare cylinder, where one can see the significant distortion of incident field caused by such a cylinder of large electrical size. The small distance between the impedance surface and the cylinder considered in this scenario, just 0.01 wavelengths, demonstrates the unique potential of the proposed approach to realize extremely thin, yet ideal cloaks, suited for electrically-large objects, in contrast with conventional passive cloaking techniques.

Similarly to its 1D *PT*-symmetric counterparts [17]-[19], the proposed cloak exhibits strong scattering asymmetry for opposite incidence directions: although the scattering is identically zero for incidence from the $+x$ direction, it becomes very large for incidence from the opposite one. As recently demonstrated [36], such an asymmetry cannot be produced by just geometrical asymmetries, but it inherently requires loss and/or gain, as in *PT*-symmetric structures. Fig. 3 presents the electric field and power distributions for the fully-cloaked cylinder of Fig. 2, but for incidence from the opposite ($-x$) direction than in Fig. 2: the incident wave experiences significant scattering, with the scattered field being over ten times larger in magnitude than the incident field. Most of the scattered energy originates from the gain portion of the metasurface, which locally sustains an infinite reflection coefficient, as discussed above, and it overwhelms the impinging signal. Consistent with the general findings in [36], reciprocity requires that the total extinction power P_{ext} of the object, integrated over all angles, is necessarily the same for both illumination directions. For propagation in the $+x$ direction, the presence of balanced loss and gain in an asymmetric distribution ensures that $P_{\text{ext}} = P_{\text{abs}} = P_{\text{scat}} = 0$, where P_{scat} is the

integrated scattered power and P_{abs} is the net absorbed power (positive and negative along the lossy and active sides) by the metasurface. Therefore, the total extinction power should also be zero when illuminated from the $-x$ direction, as in Fig. 3, leading to $P_{\text{ext}} = P_{\text{abs}} + P_{\text{scat}} = 0$ and $P_{\text{scat}} = -P_{\text{abs}}$. Notice that P_{scat} can be very large, solely sustained by the gain of the metasurface.

While the scattering cross-section is drastically different for opposite excitations, Fig. 4 shows that the scattering pattern behaves smoothly for intermediate incidence angles φ_{inc}, measured with respect to the $+x$ axis, ensuring a robust angular response of the cloak. As expected, scattering is very small in the case $\varphi_{\text{inc}} = 0°$, for which the cloak was designed, although not identically zero due to the approximation made in Eq. (2). As φ_{inc} increases, the scattering correspondingly increases, but it remains confined towards forward direction, and close to zero in the $-x$ direction for any illumination direction. This effect is a direct consequence of reciprocity: since the scattered field for a $+x$-propagating wave is essentially zero in any direction, the same should hold for the scattered field in the $-x$ direction for illumination from any other direction. A remarkable property of the patterns in Fig. 4 is that the scattering is always maximum in the $+x$ direction, with lobe broadening as φ_{inc} increases. This response is a direct consequence of the emission/reflection properties of the gain region of the surface. For small φ_{inc}, little power impinges directly on the active side of the metasurface within the ray approximation and, since all active points of the surface emit power coherently in the $+x$ direction, the scattering lobe in this direction is very narrow. On the other hand, as φ_{inc} approaches 180°, there is substantial amount of power directly hitting the gain region, resulting

in direct reflection from the surface. In this case, different points of the active region reflect in different directions, resulting in an overall broadening of the scattering lobe.

The fact that the scattering is very strong for incidence from the $+x$ direction may lead to think that the proposed cloak becomes susceptible to background electromagnetic noise or the presence of other neighboring objects. This may be true in a bi-static measurement scenario with emitter and receiver placed in the semispaces facing the passive and active sides of the cloak, respectively. In such a case, noise impinging on the structure from the $+x$ direction would be amplified by the active part of the cloak, potentially making the object recognizable. Yet, in the case of mono-static measurements, when emitter and observer are both placed on the passive side of the object, noise and scattering from neighboring objects do not affect the cloak performance, since the scattering in the $-x$ direction is zero for waves impinging from any direction, as detailed above. The scattering from the active side, and consequently the sensitivity to noise in bi-static measurements, is expected to increase as the object size grows, setting an upper limit on the size of objects that can be cloaked in a noisy environment. Scattering noise may be reduced by deviating from the zero-scattering condition; however, this would produce an analogous reduction in the amount of scattering cancelation for incidence from the $-x$ direction.

III. Simplified cloak for rhomboidal objects

Despite the apparent simplicity of Eq. (2), a non-uniform impedance profile with continuous modulation is practically challenging to achieve. Furthermore, increasing the radius of the cylinder requires using more terms in the Taylor expansion of Eq. (1), therefore further increasing the overall design complexity. This issue may seem counterintuitive considering that the approximation of a thin spacer, under which Eq. (2) was derived, becomes more accurate as

a increases, but it is the result of the large sensitivity of the gain part of the metasurface on the amplitude and phase of the cylinder's shadow fields. For these reasons, it may be highly desirable to remove spatial inhomogenities and design a metasurface that consists of only two distinct uniform regions, one with loss and another one with gain. This is possible if the object to be cloaked is confined in a rhomboidal PEC shell, as in Fig. 5, exploiting the fact that the angle between an *x*-propagating plane wave and the normal direction to the cloak surface is the same all around the shell. Notice that this is not necessarily a stringent constraint on the object shape, since a PEC shell can obviously enclose objects of any nature and shape inside it. The corners of the rhombus represent singular points, which, as it will become apparent later, have a negligible effect on the overall scattering, and can therefore be left uncloaked.

We consider a rhombus with side length a and opening angle 2θ. The mantle cloaking surface is also rhomboidal, with same opening angle and is placed at a distance d from the object to be cloaked, as shown in Fig. 4. The characteristic admittance of a TM *x*-propagating plane wave on any face of the rhombus is equal to $Y_0 \cos\theta$. Therefore, following Eq. (2), the real part of Y_s should be selected uniform as $\mathrm{Re}\{Y_s\} = Y_0 \cos\theta$ and $\mathrm{Re}\{Y_s\} = -Y_0 \cos\theta$ for the lossy and gain parts of the metasurface, respectively, so that the structure is impedance matched to *x*-propagating waves. On the other hand, $\mathrm{Im}\{Y_s\}$ should cancel the reactance of the PEC rhombus as measured at the cloaking metasurface. This reactance reads $iY_0 \cos\theta \cot(kd\cos\theta)$, as found from the expression $iY_c \cot(\beta l)$ for the input admittance of a shorted transmission line with length l, characteristic admittance Y_c and wavenumber β, after substituting $d = l$, $Y_c = Y_0 \cos\theta$ and $\beta = k\cos\theta$. Consequently, the reactive part of the surface admittance should be selected as $\mathrm{Im}\{Y_s\} = -iY_0 \cos\theta \cot(kd\cos\theta)$.

Figure 6 shows the electric field and power distribution for two electrically large rhombuses with $a = 10\lambda$ and $a = 20\lambda$, corresponding to cross-sections of 14.1λ and 28.2λ along the illumination direction. The opening angle is 90° for both cylinders and $d = 0.05\lambda$. In these cases, the cloaking admittance is only applied along the projection of the interior rhombus on the exterior one, a configuration found to minimize scattering from the edges. The case of uncloaked cylinders is also presented for comparison. It is clear that the *PT*-symmetric cloak drastically reduces reflections, scattering and shadows, even for rhomboids with very large electrical size, almost completely restoring the incident wave anywhere around the objects. The slight distortion of wave-fronts between the vertical axis of the object and its right corner is due to emission of *y*-directed plane waves by the metasurface active portion. Emission of such waves is possible because, like waves propagating along the *x*-direction, their impedance on the rhombus's faces is equal to $Y_0 \cos\theta$ and, therefore, they are locally associated with an infinite reflection coefficient along the gain part of the metasurface. Ideally, the field in the shadow region of the object would only initiate a +*x*-propagating plane wave, thus perfectly restoring the incident wave. However, the discontinuity introduced by the rhombus's corners perturbs the amplitude and phase of the shadow field, resulting in an undesired small power emission along the *y*-direction. In a practical design, elimination of this effect may be accomplished by rounding the corners of the object in an optimized fashion.

IV. Stability considerations and time evolution of the cloaking effect

The presence of an active surface with a locally infinite reflection coefficient makes the proposed cloak prone to instabilities. The fact that the active part of the surface is extended over a finite area ensures stability at the design frequency [37], as we discussed above. However, the analysis

and discussions in the previous sections were limited to steady-state monochromatic operation, and therefore stability does not necessarily hold for other frequencies or for a realistic causal excitation. A full investigation of the stability of the proposed cloak requires knowledge of the surface's admittance frequency dispersion, and therefore the assumption of a particular physical model for the admittance surface. Here we develop such a model and study the stability in the case of a circular cylindrical object, as in Fig. 1, for which analytical expressions can be derived. In addition, this analysis allows us to discuss the time evolution of the cloaking mechanism introduced here, as it reaches the steady-state condition analyzed in the previous sections.

The stability of a system can be determined from the analytical properties of its transfer function, i.e., the Fourier transform of its impulse response, in the upper half complex frequency plane ($\mathrm{Im}\{\omega\} > 0$). If the transfer function is analytic (it does not have poles or branch-points) in this plane, the system is stable. The transfer function in our case is the Green function of the cloaked object, and the corresponding poles are the resonant frequencies of the structure. Resonance frequencies are solutions of the source-free Maxwell equations, which, for the circular cylinder in Fig. 1, lead to the following expressions for the field in the space exterior and interior to the admittance surface:

$$\begin{aligned} \mathbf{E}_{\text{ext}} &= \hat{\mathbf{z}} \sum_{n=-\infty}^{\infty} c_n H_n^{(1)}(kr) e^{in\varphi}, \\ \mathbf{E}_{\text{int}} &= \hat{\mathbf{z}} \sum_{n=-\infty}^{\infty} [a_n J_n(kr) + b_n Y_n(kr)] e^{in\varphi}. \end{aligned} \tag{3}$$

The coefficients a_n, b_n and c_n can be determined from the continuity of the electric field across the surface and the admittance boundary condition $\mathbf{J}_s = Y_s \mathbf{E}_s$. After some straightforward manipulations, we find

$$J_{\mathrm{s},n} = Z_0 \sum_{m=-\infty}^{\infty} Y_{\mathrm{s},n-m} c'_m J_{s,\mathrm{m}} H_m^{(1)}(kd), \tag{4}$$

where $J_{\mathrm{s},n}$ is the n-th azimuthal harmonic of the surface current ($J_{\mathrm{s}} = \sum_{n=-\infty}^{\infty} J_{\mathrm{s},n} e^{in\varphi}$), $Y_{\mathrm{s},n}$ is the n-th azimuthal harmonic of the surface admittance ($Y_{\mathrm{s}} = \sum_{n=-\infty}^{\infty} Y_{\mathrm{s},n} e^{in\varphi}$) and

$$c'_n = -\frac{i\pi kd}{2} \frac{J_n(kd)Y_n(ka) - J_n(ka)Y_n(kd)}{H_n^{(1)}(ka)}. \tag{5}$$

The eigen-frequencies of the structure can be then calculated from the roots of the determinant of the linear system in Eq.(4).

Inspired by designs of thin metamaterial absorbers [38],[39], we propose the realization of the required admittance surface via a grating of wide metallic strips periodically loaded with lumped elements, as in Fig. 7a. If C_{g} is the capacitance between the strips and $Y_{\mathrm{L}}(\varphi)$ is the admittance of the lumped load at angular position φ, the overall surface admittance is $Y_{\mathrm{s}}(\varphi) = -i\omega C_{\mathrm{g}} + Y_{\mathrm{L}}(\varphi)$. The gap between neighboring strips is selected so that, at the design frequency ω_0, the admittance of the gap $-\omega_0 C_g$ is equal to the optimum value for $\mathrm{Im}\{Y_{\mathrm{s}}\}$ given by Eq. (2). Then, at the design frequency ω_0 the admittance of the load Y_{L} should be selected to be equal to $\mathrm{Re}\{Y_{\mathrm{s}}\}$ in Eq. (2). A possible choice for Y_{L} that satisfies this requirement is $Y_{\mathrm{L}} = -Y_0 \cos\varphi$ for the lossy part of the surface and $Y_{\mathrm{L}} = Y_0 \cos\varphi(-\omega^2 + \omega_0^2 + i\gamma\omega)/(-\omega^2 + \omega_0^2 - i\gamma\omega)$ for the active one. The lossy part simply corresponds to a passive resistor, while the interpretation of the active part requires more discussion. The active load corresponds to a negative conductance $-Y_0 \cos\varphi$ at ω_0 and a positive one $Y_0 \cos\varphi$ far from ω_0. Furthermore, at intermediate frequencies, Y_{L} has

a non-zero reactive part, as required by Kramers-Kronig relations. It should be noted that the poles of Y_L lie in the bottom half plane and, therefore, Y_L represents a bounded-input bounded-ouput (BIBO) stable element. Selection of this particular dispersion model for Y_L is based on the fact that any active system provides gain only over a limited bandwidth, which for the model used here is equal to γ. A plot of Y_L versus frequency is presented in Fig. 7b, while Fig. 7c shows a possible implementation of Y_L at radio frequencies via simple circuit elements and a negative impedance converter (NIC).

Based on the model for the surface admittance described above, Fig. 8 plots the condition number of the system in Eq. (3) for two different values of γ. The condition number is defined as the ratio between the maximum and minimum eigenvalues of the system matrix, and an infinite condition number corresponds to a zero determinant, hence an eigenmode of the structure. Results are shown only in the right half plane, since the Fourier transform is conjugate symmetric with respect to the imaginary axis, being the field quantities real in time domain. Two sets of poles can be identified, far and close to the design frequency ω_0. The poles far from ω_0 correspond to a grating loaded with a passive conductance $Y_0|\cos\varphi|$, i.e., the value of Y_L far from ω_0. As expected, these poles are always stable, since they are associated only to passive elements. On the other hand, the poles close to ω_0 are the result of the active part of Y_L. For large γ, some of these poles lie in the upper half plane, leading to an unstable system. As γ decreases, i.e., as the bandwidth over which $\mathrm{Re}\{Y_L\} < 0$ decreases, these poles move closer to the real frequency axis and they eventually enter the bottom half plane, ensuring that the system is stable. Since γ determines the bandwidth of the structure, it is evident that there is a maximum

possible bandwidth for the chosen dispersion profile to ensure stability. Increasing the size of the object leads to a decrease in the maximum available bandwidth over which the proposed configuration is stable, but increasing the complexity of the cloak with proper dispersion engineering may push forward this limit. It is interesting that, while the use of active elements may relax several of the conventional bandwidth limitations imposed by passivity, both on the absorber side and on the active side, stability requirements and the necessity to guarantee an active response impose now the fundamental limitations to an arbitrarily broadband response. It should be stressed, however, that the limit on bandwidth outlined in Fig. 8 depends on the particular dispersive model assumed for the surface admittance (both on the passive and active side), and it may be therefore significantly extended by considering other, more complex, circuit models for the cloak implementation. The model for Y_{L} used here, and the corresponding values of bandwidth, are non-optimal, and have been selected simply to demonstrate the feasibility of the proposed concept for cloaking. The determination of optimal designs to ensure large bandwidths over which stability is ensured is a dispersion-engineering problem that falls beyond the scope of the present paper.

The knowledge of the properties of the poles in the complex frequency plane allows a better understanding and provides relevant insights into the physical mechanisms at the basis of the proposed cloaking effect. For this purpose, we consider excitation with a causal pulse of semi-infinite temporal extent centered at frequency ω_0 and impinging on the structure at time zero. We recall from linear-systems theory that the electric field everywhere in space can be expressed as the superposition of the steady-state contribution analyzed in previous sections and a transient response $\mathbf{E}_{\mathrm{tr}}(\mathbf{r},t)=\sum_p A_p(\mathbf{r})e^{-i\omega_p t}$, where ω_p is the eigen-frequency of the p-th mode of the

structure and $A_p(\mathbf{r})$ the corresponding resonance amplitude, which depends on the mode profile over space and the spectral content of the incident pulse [40]. Consider first a cylinder covered only from its left-hand side with a matched lossy surface, as in Fig. 2a. In such a case, the eigen-spectrum of the structure consists of the modes far from ω_0 in Fig. 8. Since the imaginary parts of the eigen-frequencies of these modes are large negative numbers, the transient effect is expected to be short, and a steady state is expected to be quickly established, when all the incident power is absorbed and a large shadow is created at the opposite (non-covered) side of the cylinder, as in Fig. 2a. The transient effect primarily consists of reflection of the incident pulse wavefront, due to its finite bandwidth, and to the dispersion of the lossy side of the cloak [41].The response of a fully covered cylinder, with both lossy and active portions of the surface, is not very different at early times after the wave hits the object, when the response of the structure is primarily determined by the poles far from ω_0 in Fig. 8. However, as time progresses, the resonant eigen-states of the cloak close to ω_0 in Fig. 8, sustained by the active side, are excited and dramatically change the overall field distribution. For a stable structure, as in Fig. 8b, these states eventually decay to zero, since they are associated with poles in the bottom half plane. However, in the meanwhile, these modes are responsible for sustaining the coupling between passive and active sides of the surface, establishing the necessary amplitude and phase conditions on the active part of the admittance surface to generate the desired fields, in sync with the wavefront impinging the object, effectively canceling the shadow and forward scattering. In a sense, the eigen-modes of the system assist the incident wave to establish the appropriate conditions on the active part of the surface for restoration of the incident field in the forward direction in the steady-state. Due to causality, there will always be a finite transient regime over which the cloaked object will be visible, but the presence of active components in

the cloak, and suitable dispersion engineering of the surface, may provide tools to ensure that the cloak reaches the steady-state response in a relatively short transient time, allowing for broadband operation.

V. Discussion and conclusions

The structure presented in this paper shares some limited, yet interesting connections with the ones introduced in Refs. [15],[16]. In particular, for incidence from the left (ideal invisibility case) the steady-state electric current distribution induced on the passive/active metasurface is equivalent to the magnetic current distribution derived in Ref. [15]. This is to be expected, recalling that an electric current at close distance from a PEC plane is equivalent to a magnetic current directly on the plane and that, due to the equivalence principle, there is a unique current distribution that makes an object ideally invisible. However, there are fundamental differences regarding the physical mechanism leading to the cloaking effect between the approach presented here and the scheme introduced in [15]. Cloaking in [15] is achieved by surrounding the cylinder with a series of independent magnetic loop antennas which collectively radiate a field opposite to the scattered field by the bare cylinder. The amplitudes and phases of the signals feeding the loop antennas need to be a precise function of the incident wave and, as a result, a change in amplitude, phase or position of the source requires a change in the amplitudes and phases of the feeding signals through an active feedback system. In a sense, the problem in [15] is the superposition of two independent problems, which, under specific conditions, can interfere destructively and result in scattering cancelation. On the other hand, the proposed passive/active metasurface automatically adapts and synchronizes in an autonomous fashion the induced surface current distribution to the incident field through the resonant states of the metasurface, as if the structure presented an internal feedback mechanism that allows to unidirectionally cloak

the object, for any amplitude and phase of the impinging wave, tracking in real time the impinging signal. Even a modulated signal within the operational bandwidth of the cloak would go through the obstacle with minimal distortion or scattering. The eigen-modal radiation sustained by the active part is fed by the passive portion of the metasurface through their wave interaction, and the combination of the two provides a unique way of ideal unidirectional cloaking.

Similar to our approach, the one presented in Ref. [16] is also based on the concept of absorbing incident power from one side of the cloaked object and re-emitting it from the other side of the object. To this end, Ref. [16] relies on a complex feedback mechanism between the absorbing and emitting parts of the cloak, different than the natural feedback mechanism through wave propagation around the cloak on which our technique is based, which allows making an object invisible to arbitrary pulses impinging from arbitrary directions, however at the expense of intensive signal processing and requirement of complicated networks of sensors and sources. On the other hand, our approach is based on relatively simple active metasurfaces, able to make an object invisible to signals impinging from a particular direction by exploiting the natural feedback mechanism established through wave propagation around the object, thus not requiring any computationally-expensive signal-processing operation.

Our work shows that balanced loss and gain, such as in *PT*-symmetric systems, can open exciting new venues to cloak objects much larger than the wavelength. Our approach essentially extends the conventional stealth approaches to camouflaging, showing that, by employing a time-reversed version of an ideal stealth surface on the opposite side of the object, one can realize a super-stealth configuration that can fully eliminate the object scattering. The coating surface fully absorbs the impinging power on one side of the object and at the same time emits

the required radiation from the other side. Similar to 1D *PT*-symmetric lattices, the structure exhibits strong scattering asymmetry: for one propagation direction it is invisible, while for the opposite one it exhibits significant back-scattering. While this work has focused on 2D objects, similar principles can be straightforwardly extended to 3D. We conclude pointing out that a similar scheme can be applied to objects of arbitrary, asymmetric shape and/or to impinging waves of arbitrary form. By breaking the spatial symmetries assumed in this paper, the required metasurface, while still retaining balanced loss-gain features, will not be *PT*-symmetric, to allow proper compensation of the asymmetries in the object or in the excitation.

This work was supported by AFOSR with grant No. FA9550-13-1-0204 and the NSF CAREER award No. ECCS 0953311.

References

[1] N. Engheta and R. W. Ziolkowski, *Metamaterials: Physics and Engineering Explorations* (John Wiley & Sons, 2006).

[2] J. B. Pendry, D. Schurig, and D. R. Smith, Controlling Electromagnetic Fields, Science **312**, 1780 (2006).

[3] D. Schurig, J. J. Mock, B. J. Justice, S. A. Cummer, J.B. Pendry, A. F. Starr, and D. R. Smith, Metamaterial electromagnetic cloak at microwave frequencies, Science **314**, 977 (2006).

[4] A. Alù and N. Engheta, Achieving transparency with plasmonic and metamaterial coatings, Phys. Rev. E **72**, 016623 (2005).

[5] A. Alù, Mantle cloak: Invisibility induced by a surface, Phys. Rev. B **80**, 245115 (2009).

[6] P. Y. Chen, J. Soric, and A. Alù, Invisibility and Cloaking Based on Scattering Cancellation, Adv. Mater. **24**, OP281 (2012).

[7] J. C. Soric, P. Y. Chen, A. Kerkhoff, D. Rainwater, K. Melin, and A. Alù, Demonstration of an ultralow profile cloak for scattering suppression of a finite-length rod in free space, New J. Phys. **15**, 033037 (2013).

[8] F. Monticone and A. Alù, Do cloaked objects really scatter less?, Phys. Rev. X **3**, 041005 (2013).

[9] H. Hashemi, C.-W. Qiu, A. P. McCauley, J. D. Joannopoulos, and S. G. Johnson, Diameter-bandwidth product limitation of isolated-object cloaking, Phys. Rev. A 86, 013804 (2012).

[10] B. Zhang, Y. Luo, X. Liu, and G. Barbastathis, Macroscopic invisibility cloak for visible light, Phys. Rev. Lett. **106**, 033901 (2011).

[11] X. Chen, Y. Luo, J. Zhang, K. Jiang, J. B. Pendry, and S. Zhang, Macroscopic invisibility cloaking of visible light, Nat. Commun. **2**, 176 (2011).

[12] N. Landy and D. R. Smith, A full-parameter unidirectional metamaterial cloak for microwaves, Nat. Mater. **12**, 25 (2013).

[13] M. Selvanayagam and G. V. Eleftheriades, An active electromagnetic cloak using the equivalence principle, IEEE Antennas Wireless Propag. Lett. **11**, 1226 (2012).

[14] M. Selvanayagam and G. V. Eleftheriades, Discontinuous electromagnetic fields using orthogonal electric and magnetic currents for wavefront manipulation, Opt. Express **21**, 14409 (2013).

[15] M. Selvanayagam and G. V. Eleftheriades, Experimental demonstration of active electromagnetic cloaking, Phys. Rev. X **3**, 041011 (2013).

[16] D. A. B. Miller, On perfect cloaking, Opt. Express **14**, 12457 (2006).

[17] Z. Lin, H. Ramezani, T. Elchelkraut, T. Kottos, H. Cao, and D. N. Christodoulides, Unidirectional invisibility induced by *PT*-symmetric periodic structures, Phys. Rev. Lett. **106**, 213901 (2011).

[18] A. Mostafazadeh, Invisibility and *PT* symmetry, Phys. Rev. A **87**, 012103 (2013).

[19] L. Feng, Y.-L. Xu, W. F. Fegadolli, M.-H. Lu, J. E. B. Oliveira, V. R. Almeida, Y.-F. Chen, and A. Scherer, Experimental demonstration of a unidirectional reflectionless parity-time metamaterial at optical frequencies, Nat. Mater. **12**, 108 (2013).

[20] X. Yin and X. Zhang, Unidirectional light propagation at exceptional points, Nat. Mater. **12**, 175 (2013).

[21] C. M. Bender and S. Boettcher, Real spectra in non-Hermitian Hamiltonians having *PT* symmetry, Phys. Rev. Lett. **80**, 5243 (1998).

[22] C. M. Bender, Making sense of non-Hermitian Hamiltonians, Rep. Prog. Phys. **70**, 947 (2007).

[23] Y.-C. Lee, M.-H. Hsieh, S. T. Flammia, and R.-K. Lee, Local *PT* symmetry violates the no-signaling principle, Phys. Rev. Lett. **112**, 130404 (2014).

[24] K. G. Makris, R. El-Ganainy, D. N. Christodoulides, and Z. H. Musslimani, Beam dynamics in *PT* symmetric optical lattices, Phys. Rev. Lett. **100**, 103904 (2008).

[25] C. E. Rüter, K. G. Makris, R. El-Ganainy, D. N. Christodoulides, M. Segev, and D. Kip, Observation of parity-time symmetry in optics, Nat. Phys. **6**, 192-195 (2010).

[26] A. Guo, G. J. Salamo, D. Duchesne, R. Morandotti, M. Volatier-Ravat, V. Aimez, G. A. Siviloglou, and D. N. Christodoulides, Observation of *PT*-symmetry breaking in complex optical potentials, Phys. Rev. Lett. **103**, 093902 (2009).

[27] A. Regensburger, C. Bersch, M.-A. Miri, G. Onishchukov, D. N. Christodoulides, and U. Peschel, Parity-time synthetic photonic lattices, Nature **488**, 167 (2012).

[28] Y. D. Chong, L. Ge, and A. D. Stone, *PT*-symmetry breaking and laser-absorber modes in optical scattering systems, Phys. Rev. Lett. **106**, 093902 (2011).

[29] F. Nazari, N. Bender, H. Ramezani, M. K. Moravvej-Farshi, D. N. Christodoulides, and T. Kottos, Optical isolation via *PT*-symmetric nonlinear Fano resonances, Opt. Express **22**, 9574 (2014).

[30] B. Peng, Ş. K. Özdemir, F. Lei, F. Monifi, M. Gianfreda, G. L. Long, S. Fan, F. Nori, C. M. Bender, and L. Yang, Parity-time-symmetric whispering-gallery microcavities, Nat. Phys. **10**, 394 (2014).

[31] R. Fleury, D. L. Sounas, and A. Alù, Negative refraction and planar focusing based on parity-time symmetric metasurfaces, Phys. Rev. Lett. **113**, 023903 (2014).

[32] R. Fleury, D. L. Sounas, and A. Alù, An invisible acoustic sensor based on parity-time symmetry, Nature Commun. **6**, 5905 (2015).

[33] X. Zhu, L. Feng, P. Zhang, X. Yin, and X. Zhang, One-way invisible cloak using parity-time symmetric transformation optics, Opt. Lett. **38**, 2821 (2013).

[34] X. Zhu, H. Ramezani, C. Shi, J. Zhu, and X. Zhang, *PT*-Symmetric Acoustics, Phys. Rev. X **4**, 031042 (2014).

[35] P. Y. Chen, C. Argyropoulos, and A. Alù, Broadening the cloaking bandwidth with non-Foster metasurfaces, Phys. Rev. Lett. **111**, 233001 (2013).

[36] D. L. Sounas and A. Alù, Extinction symmetry for reciprocal objects and its implications on cloaking and scattering manipulation, Opt. Lett. **39**, 4053 (2014).

[37] The worst case scenario at the design frequency in terms of stability arises when we excite the cloak with a plane wave propagating in the –*x* direction, *i.e.*, a wave directly impinging on the gain side of the surface from a direction corresponding to a locally infinite reflection coefficient. An infinite planar surface with such a property would indeed exhibit a globally infinite reflection coefficient, and therefore would be inherently unstable. However, in the case of a finite circular cylinder, the area covered by the gain medium is limited, and the curvature of the surface disperses the scattered power all over space, resulting in a finite and fully stable scattering response. This fact is verified by the scattering patterns in Fig. 4: although the scattered power increases as the incidence angle increases, it is always finite.

[38] N. Engheta, Thin absorbing screens using metamaterial surfaces, in 2002 IEEE AP-S Int. Symp. Dig. **2**, 392 (2002).

[39] S. A. Tretyakov and S. I. Maslovski, Thin absorbing structure for all incidence angles based on the use of a high-impedance surface, Microw. Opt. Technol. Lett. **38**, 175 (2003).

[40] J. D. Van Bladel, *Electromagnetic fields* (John Wiley & Sons, New Jersey, 2007).

[41] The finite bandwidth of the lossy part of the cloak can be easily understood in the case of Fig. 7a. The effective surface admittance on the outer surface of the cloak is $Y_{\mathrm{L}} - i\omega C_{\mathrm{g}} + Y_{\mathrm{cyl}}$, where Y_{cyl} is the admittance of the metallic cylinder (the cloaked object). According to the design, Y_{L} is real and matched to the impinging wave while $-i\omega C_{\mathrm{g}}$ cancels Y_{cyl} at frequency ω_0. It is obvious that the structure is perfectly matched to incident waves only at ω_0, although good matching can also be expected in a limited band around this frequency. By considering active components also on this side of the

surface, it may be possible to overcome these limitations and significantly broaden this bandwidth of operation.

Figures

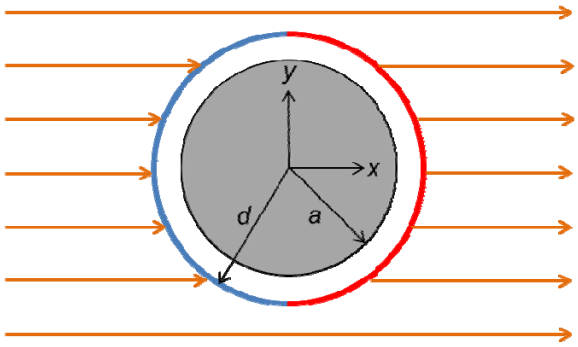

Fig. 1. A perfectly conducting cylinder covered by a *PT*-symmetric surface. The left and right portions of the surface (blue and red in the figure) have loss and gain, respectively. The lossy part is tailored to absorb all of the impinging power, the gain part emits the same amount of power, synchronized to the impinging signal.

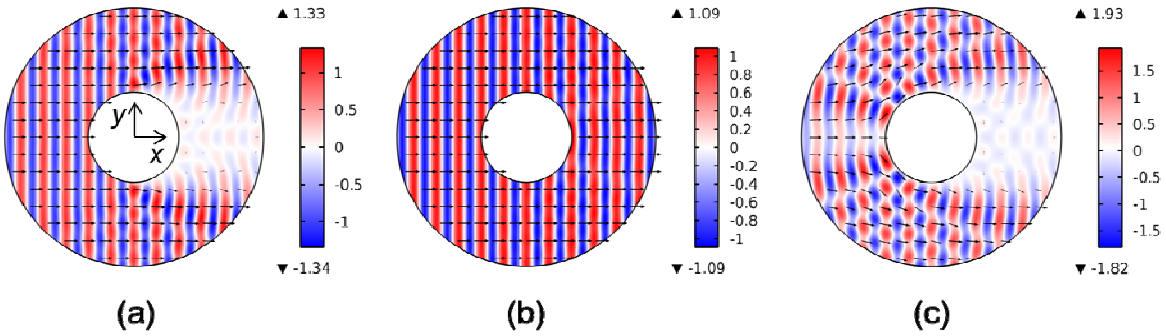

Fig. 2. Total electric field (color plot, snapshot in time, normalized to the incident amplitude) and power (vectorial plot) distribution for a PEC cylinder with $a = 2\lambda$. The structure is illuminated from its left-hand side. (a) The cylinder is covered only on its left-hand side with a lossy impedance following Eq. (2) for $|\varphi| > \pi/2$. The distance between the impedance and the cylinder is 0.01λ. (b) Fully-cloaked cylinder using the *PT*-symmetric impedance surface described by Eq. (2). (c) Cylinder without cloak.

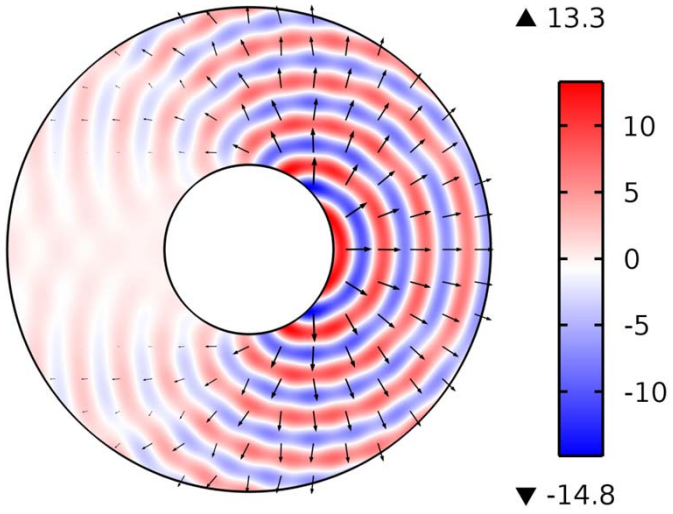

Fig. 3. Similar to Fig. 2b, but for incidence from $-x$. Total electric field (color plot, snapshot in time, normalized to the incident amplitude) and power (vectorial plot) distribution for a *PT*-symmetric cloaked circular cylinder with radius $a = 2\lambda$. The thickness of the spacer between the cloaking metasurface and the cylinder is again $d - a = 0.01\lambda$.

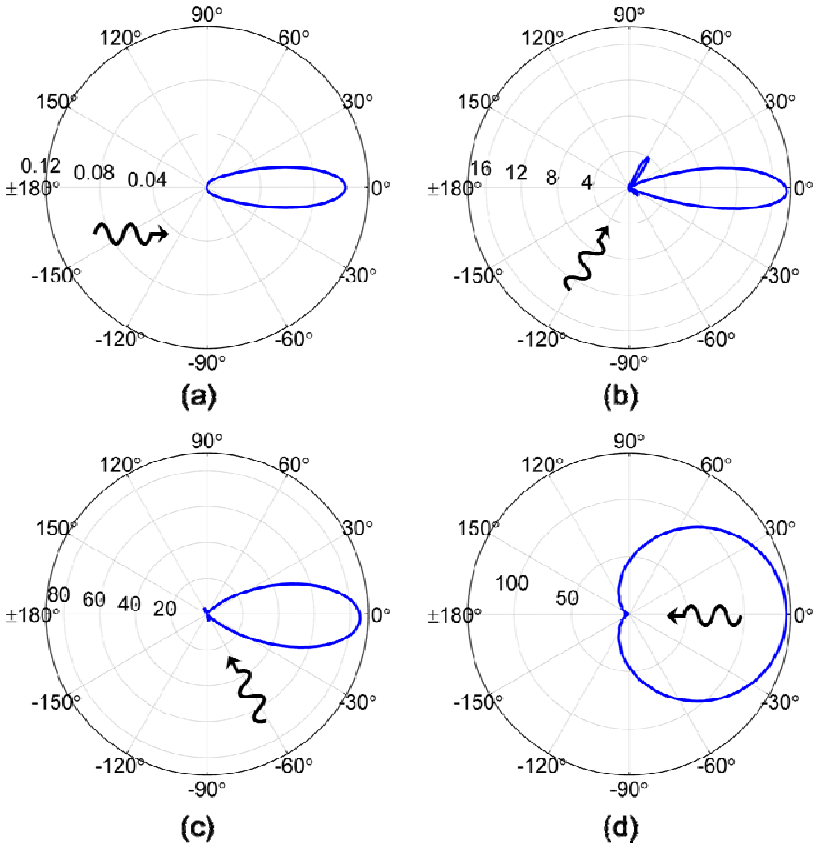

Fig. 4. Calculated scattering cross-section for the *PT*-symmetric cloaked cylinder of Fig. 2b versus the azimuthal angle φ for different incidence angles, φ_{inc}: (a) $\varphi_{\text{inc}} = 0°$, (b) $\varphi_{\text{inc}} = 60°$, (c) $\varphi_{\text{inc}} = 120°$ and (d) $\varphi_{\text{inc}} = 180°$. The radius of the cylinder is $a = 2\lambda$ and the separation between the metasurface and the cylinder $d - a = 0.01\lambda$. The results are normalized to the total scattering cross-section of the bare cylinder.

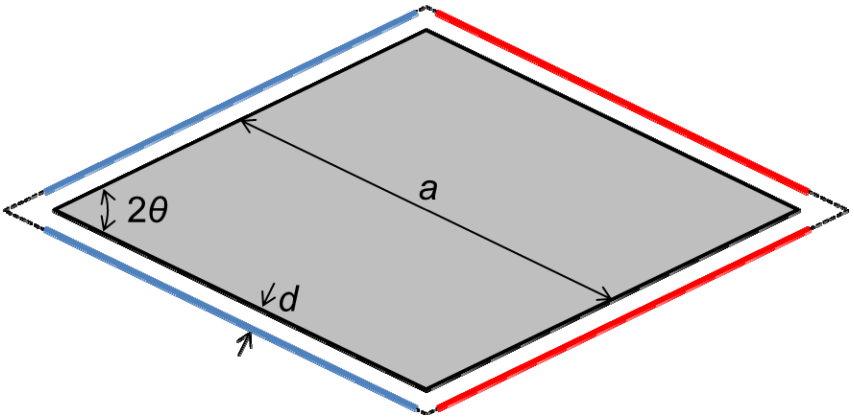

Fig. 5. PEC rhomboidal cylinder covered with a conformal *PT*-symmetric metasurface in the form of a rhomboidal cylinder with same opening angle. As in the case of the circular cylinder, the left and right portions of the metasurface have loss and gain, respectively, in order to absorb and emit plane waves impinging from the left. The *PT* cloak is only applied to the projection of the PEC rhombus on the outer rhombus, indicated with dashed line.

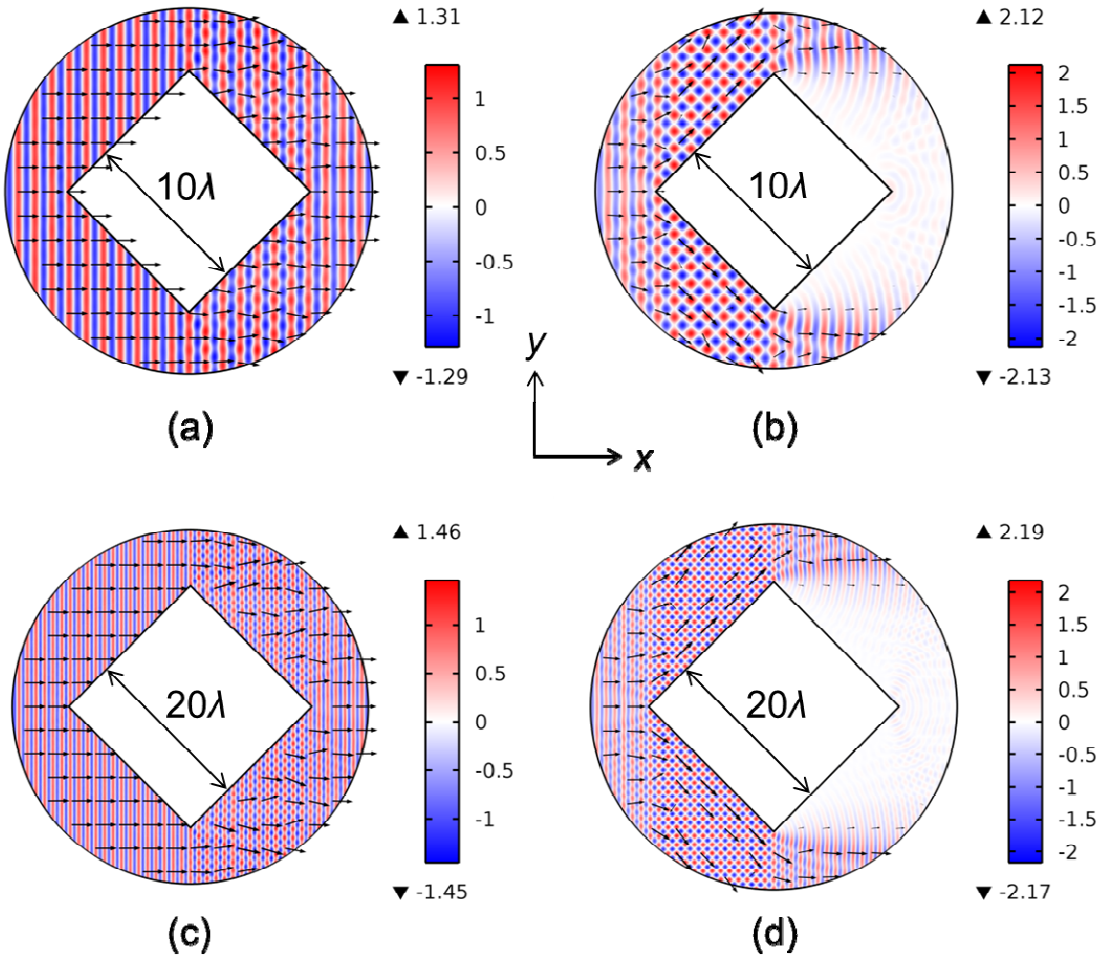

Fig. 6. Electric field (color plot) and power (vectorial plot) distribution in the case of a PEC rhomboid with an opening of $90°$. (a) *PT*-symmetric-cloaked rhomboid with $a = 10\lambda$ and $d = 0.05\lambda$. (b) Bare rhomboid with $a = 10\lambda$. (c) *PT*-symmetric-cloaked rhomboid with $a = 20\lambda$ and $d = 0.05\lambda$. (d) Bare rhomboid with $a = 20\lambda$.

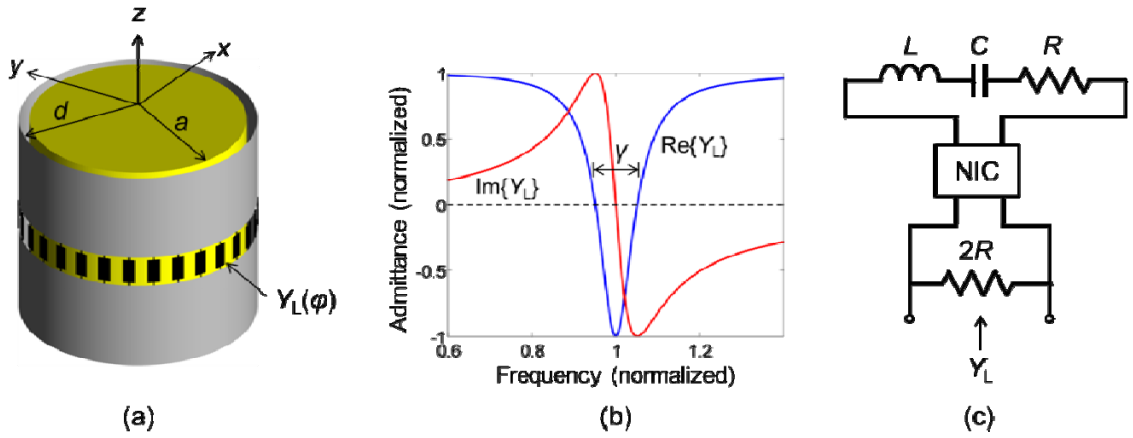

Fig. 7. Physical implementation of the *PT*-symmetric cloak in the case of a circular cylinder. (a) Realization of the admittance surface via a grating of wide metallic strips periodically loaded with lumped elements $Y_{\mathrm{L}}(\varphi)$. (b) Real and imaginary part of Y_{L} versus frequency. (c) Circuit implementation of Y_{L} at radio frequencies via simple circuit elements and a negative impedance converter (NIC). The values of the elements are: $R = 1/[2Y_{\mathrm{L}}(\omega_0)]$, $L = R/\gamma$ and $C = 1/(\omega_0^2 L)$.

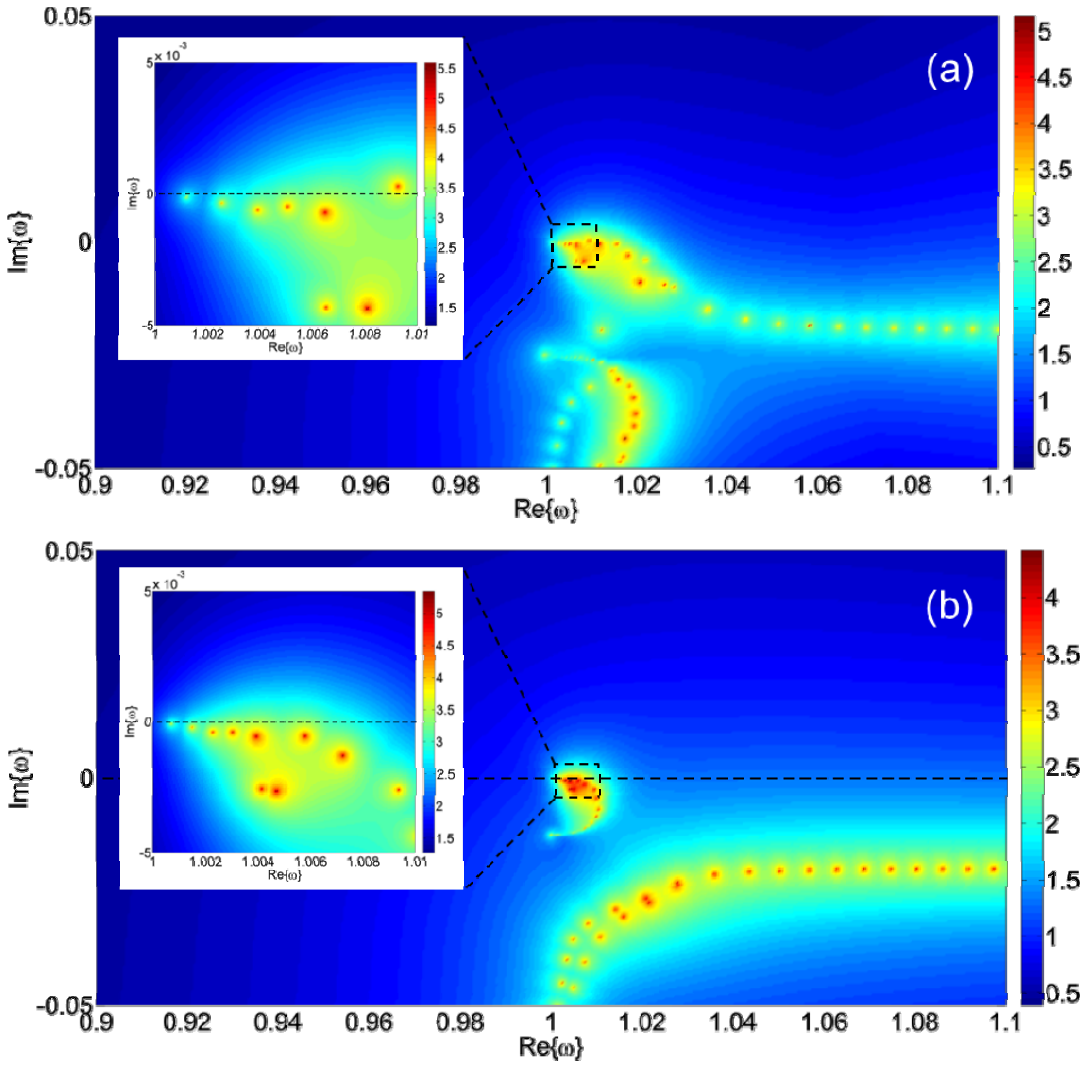

Fig. 8. Condition number of the system in Eq. (3) for a circular cylinder with $a = \lambda_0$ and $d - a = 0.01\lambda_0$. The admittance surface is implemented as in Fig. 7. (a) $\gamma = 0.05$. A pole can be found in the upper half-plane and, therefore, the system is unstable. (b) $\gamma = 0.005$. All the poles lie in the bottom half plane, indicating a stable system.